Quaternary Science Reviews 312 (2023) 108162

Contents lists available at ScienceDirect

Quaternary Science Reviews

journal homepage: www.elsevier.com/locate/quascirev

Bipolar ice-core records constrain possible dates and global radiative forcing following the ~74 ka Toba eruption

Jiamei Lin [a, *], Peter M. Abbott [b], Michael Sigl [b], Jørgen P. Steffensen [a], Robert Mulvaney [c], Mirko Severi [d], Anders Svensson [a, **]

[a] Physics of Ice, Climate and Earth, Niels Bohr Institute, University of Copenhagen, 2100, Denmark
[b] Climate and Environmental Physics, Physics Institute & Oeschger Center for Climate Change Research, University of Bern, Sidlerstrasse 5, Bern, Switzerland
[c] British Antarctic Survey, Cambridge, UK
[d] Department of Chemistry, University of Florence, Florence, Italy

ARTICLE INFO

Article history:
Received 1 May 2022
Received in revised form
21 May 2023
Accepted 28 May 2023
Available online xxx

Handling Editor: Giovanni Zanchetta

Keywords:
Younger toba tuff eruption
Ice cores
Volcanic sulfur emission strength
Volcanic radiative forcing

ABSTRACT

The Younger Toba Tuff eruption ~74 ka ago in Indonesia, is among the largest known supereruptions in the Quaternary and its potential impact on the climate system and human evolution remains controversially debated. The eruption is dated radiometrically to 73.88 ± 0.32 ka (1σ, Storey et al., 2012) and it occurred at the abrupt cooling transition from Greenland Interstadial 20 to Greenland Stadial 20. The precise stratigraphic position of volcanic fallout detected in ice cores from both polar ice sheets has previously been narrowed down to four potential candidates. Here, we compile all available Greenland and Antarctic sulfate records, together with electrical conductivity records and recently obtained sulfur isotope records to identify, quantify and characterize these Toba candidates in terms of their likely latitudinal position of eruption, sulfur emission strength and radiative forcing. We identify that the youngest event of the four candidates is composed of two separate eruptions, both likely located in the extra-tropical Northern Hemisphere. We deem the two older events unlikely candidates for the Toba eruption because of their limited sulfur emission strengths. The second youngest event has the largest sulfur output of the Toba candidates, and it is also larger than any other volcanic event identified in ice core records over the last 60 kyr. Comparable amounts of sulfate deposits in Greenland and Antarctica strongly suggest a tropical source. We thus propose the second youngest event (74,156 years before 2000 CE) to be most likely associated with the Toba eruption. The estimated stratospheric sulfate loading of the proposed Toba eruption is 535 ± 96 Tg, which is 3 times that of Samalas 1258 CE, 6 times that of Tambora (1815) CE and 20 times that of Pinatubo (1991) CE. We derive the continuous time-series of volcanic sulfate deposition, sulfur emission strength and radiative forcing over the 74.8–73.8 ka time window, suitable for conducting experiments with climate models that either require prescribed forcing field or interactively reproduce aerosol processes. We estimate the cumulative volcanic sulfur emission strength and the radiative forcing of the two younger events and they are found to be much stronger than those at the onset of the Younger Dryas and those preceding the Little Ice Age. Stacked Greenland water isotope records show an accelerated transition trend and abrupt shift after the proposed Toba eruption and suggest that the Greenland moisture source moved southward shortly after the Toba eruption. The Toba eruption may thus have an amplifying effect on the cooling transition leading to Greenland Stadial 20.

© 2023 The Authors. Published by Elsevier Ltd. This is an open access article under the CC BY license (http://creativecommons.org/licenses/by/4.0/).

1. Introduction

The Youngest Toba Tuff (Toba) eruption in Indonesia is among the largest known supereruptions over the past 2.5 million years with 2500–3000 km^3 of magma deposited (Chesner et al., 1991; Rose et al., 1987). The eruption has been precisely dated by ^{40}Ar/^{39}Ar to 73.88 ± 0.32 ka in Malaysia (1σ, Storey et al., 2012) and at 73.7 ± 0.3 ka in India (1σ, Mark et al., 2017). Ash from the eruption has been widely discovered in marine sediments from the Arabian Sea (Von Rad et al., 2002), the Indian Ocean (Shane et al.,

* Corresponding author.
** Corresponding author.
E-mail addresses: jm.lin@nbi.ku.dk (J. Lin), as@nbi.ku.dk (A. Svensson).

https://doi.org/10.1016/j.quascirev.2023.108162
0277-3791/© 2023 The Authors. Published by Elsevier Ltd. This is an open access article under the CC BY license (http://creativecommons.org/licenses/by/4.0/).

1995) and the South China Sea (Song et al., 2000; Huang et al., 2001; Liu et al., 2006; Buhring and Sarnthein, 2000), in lake sediments from Lake Malawi in Africa (Lane et al., 2013), and across the Indian subcontinent (Pearce et al., 2014). Although, to date, no tephra has been identified in ice cores (Abbott et al., 2012), the ash layers identified in the marine sediment records of the Arabian Sea strongly suggest that the eruption occurred at the cooling transition from Greenland Interstadial 20 (GI-20) to Greenland Stadial 20 (GS-20) (Schulz et al., 1998; Deplazes et al., 2013). In this interval, four volcanic sulfate events identified in both Greenland and Antarctic ice cores have been proposed as Toba candidates (named T1, T2, T3 and T4; Svensson et al., 2013). These are dated to 74,057, 74,156, 74,358 and 74,484 a b2k, respectively, using the Greenland GICC05modelext time scale (Wolff et al.2010). Recently, sulfur isotope analysis of Antarctic ice cores suggested that the T1 and T2 events are the most likely candidates for the Toba eruption (Crick et al., 2021).

A large explosive eruption can heavily disturb the regional and global climate through direct radiative impact of the stratospheric sulfate aerosol burden and also through feedbacks involving oceanic and atmospheric circulation (Robock, 2000; Pausata et al., 2015; McConnell et al., 2020; Sigl et al., 2015). It has been suggested that the Toba eruption is associated with a human population bottleneck that occurred in the period between 50 and 100 ka (Rampino and Self, 1993; Ambrose, 1998). However, this hypothesis has been challenged as continued human activity is suggested (Ge and Gao, 2020), and modern humans appeared not to be strongly impacted by the Toba eruption at a South African site (Smith et al., 2018; Jackson et al., 2015) as well as in India (Clarkson et al., 2020; Mark et al., 2014), which indicates that the impact on those areas may have been less severe.

The magnitude of the stratospheric sulfate loading from past eruptions, commonly derived from reconstructing volcanic sulfate deposition on the polar ice sheets, is key to estimating the cooling effect of past eruptions. For volcanic eruptions that occurred in the last 2500 years, Sigl et al. (2015) established a strong relationship between the reconstructed post-eruption temperature cooling estimated from tree-ring records and the enhanced stratospheric sulfate aerosol burden estimated from ice cores. The sulfur emission strength of the Toba eruption, estimated using petrological evidence, has a wide range from 105 Tg to 9900 Tg, that is almost 4 to 396 times that of the Mt Pinatubo 1991 CE eruption (Chesner and Luhr, 2010; Scaillet et al., 1998; Oppenheimer, 2002; Quaglia et al., 2023). The debate regarding the climatic consequences of the Toba eruption is strongly tied to the poorly constrained sulfur emission strength in model simulations. Model simulations of the Toba eruption applying 5–900 times the SO_2 emission of the 1991 CE Pinatubo eruption used the idealized stratospheric chemistry or aerosol micro-physics mechanism and suggested a 2.3–17.0 °C mean global cooling following the eruption (Osipov et al., 2020; Black et al., 2021; Robock et al., 2009), in comparison to the ~0.5 °C global cooling following the 1991 CE Pinatubo eruption (Parker et al., 1996).

Whether a single volcanic eruption could have triggered abrupt climate change, such as the onset of Dansgaard-Oeschger (DO) events in glacial periods (Lohmann and Svensson, 2022; Baldini et al., 2015), have accelerated the deglaciation in the Southern Hemisphere (Mcconnell et al., 2017), or whether a cluster of volcanic eruptions could lead to an extended period of climate cooling and ice growth (Abbott et al.; Miller et al., 2012) are topics currently being debated. Pinpointing the precise position of the Toba eruption in the cooling transition leading to GS-20 will help to explore these questions and to decipher the mechanisms involved. A recent re-dating of the Los Chocoyos eruption (LCY) of Atitlán volcano in present day Guatemala suggests that this eruption occurred at 75 ± 2 ka (Cisneros de Leon et al., 2021) opening the possibility that two supereruptions occurred close to the onset of GS-20 and, in combination, could have triggered the GS-20 cooling (Paine et al., 2021). However, this new date is at odds with the commonly accepted age of the 84 ka BP (Brenna et al., 2020) based on isotope profile matching of the respective tephra layer in marine records (Drexler et al., 1980) and thus warrants further investigations.

In this study, we compile all available sulfate, conductivity and electrical conductivity measurement (ECM) records from Greenland and Antarctic ice cores to reassess the Toba candidates and estimate the associated volcanic sulfate deposition in Greenland and Antarctica. Sulfate records from four Greenland and two Antarctic ice cores are firstly utilised to derive the volcanic sulfate deposition. Although Toba candidates have been previously identified from polar ice cores (Svensson et al., 2013) and the ice-core sulfur isotope signal has been used to indicate the altitude of eruption plume (Crick et al., 2021), the exact position of the Toba eruption in the ice-core records has not been determined. Here, we predict the latitudinal locations of candidate eruptions based on the method of Lin et al. (2022) and use the sulfur emission strength from our reconstruction to pinpoint the Toba eruption. Furthermore, we reconstruct sequences of the sulfur emission strengths and the spatial-temporal volcanic radiative forcing at the cooling transition to GS-20 (74.8–73.8 ka b2k) using the synchronized sulfate records of Greenland and Antarctic ice cores. Unless otherwise stated, all ages in this study are referring to the model extended Greenland Ice Core Chronology 2005 (GICC05) (Rasmussen et al., 2014) using the datum 2000 AD (b2k).

2. Methods

We employed five sulfate records from four Greenland ice cores – an Ion Chromatography (IC) sulfate record of the Greenland Ice Core Project (GRIP) ice core (this work), a Fast Ion Chromatography (FIC) sulfate record from the North Greenland Eemian Ice Drilling (NEEM) ice core (Schüpbach et al., 2018), a Continuous Flow Analysis (CFA) record from the North Greenland Ice Core Project (NGRIP) ice core (Svensson et al., 2013) and two IC sulfate records from the Greenland Ice Sheet Project 2 (GISP2) ice core (Mayewski et al., 1997; Yang et al., 1996). Four sulfate records from two Antarctic ice cores are used - two records measured by FIC and IC from the EPICA Dome C (EDC) ice core (Crick et al., 2021; Svensson et al., 2013) and two records measured by FIC and IC from the EPICA Dronning Maud Land (EDML) ice core (Svensson et al., 2013; Crick et al., 2021) (Fig. S1, Table 1 and Table S1). From those records, we reconstruct volcanic sulfate deposition on the ice sheets for the period 74,800–73,800 a b2k (Fig. S2 and Table S2). For Greenland, the effective time resolution of the sulfate measurements is 1–2 years for NGRIP (Svensson et al., 2013), 1–5 years for GISP2 (Yang et al., 1996), 5–10 years for GRIP (this work), 10 years for NEEM (Schupbach et al., 2018) and 50–150 years for GISP2 (Mayewski et al., 1997). For Antarctica, the temporal time resolution of EDML and EDC sulfate measurements fall in the range of 1–3 years (Svensson et al., 2013). The EDML and EDC sulfate records from Crick et al. (2021) were solely sampled for the Toba candidate peaks, as identified by Svensson et al. (2013), at a 1–8 year temporal resolution. Due to the magnitude of the Toba candidates, those events are detectable in sulfate records of lower temporal resolution.

Using the T1-T4 Toba candidates identified in the NGRIP, GRIP, GISP2, EDC and EDML ice cores by Svensson et al. (2013), we linearly interpolated the GICC05 time scale for the period of 74.8–73.8 ka b2k for those cores. For the NEEM core, we apply the volcanic synchronization between the NEEM and NGRIP cores (Rasmussen et al., 2013) to identify the Toba candidates in NEEM and make a

Table 1
Detailedinformationabout volcanicage, depth,sulfatebackground, sulfatedeposition,effectivetimetemporalresolution,ice-coresiteflowmodeland estimateduncertaintyforindividualTobacandidateinpolaricecores.

Ice Core	Record	T1a							T1b						
		Start age	End age	Depth	Bckgrd	Thinning	Deposition	Uncertainty	Start age	End age	Depth	Bckgrd	Thinning	Deposition	Uncertainty
		a b2k	a b2k	m	ppb		kg km^{-2}	kg km^{-2}	a b2k	a b2k	m	ppb		kg km^{-2}	kg km^{-2}
EDC (Svenssonet al., 2013)	FIC SO4								74,048	74,063	1078.96	170.3	0.64	56.0	22.4
EDC (Crick et al., 2021)	ICPMS								74,042	74,071	1078.95	230.4	0.64	65.0	26.0
EDML (Svenssonet al., 2013)	FIC SO4								74,050	74,065	1866.62	106.5	0.28	108.0	43.2
EDML (Crick et al., 2021)	ICPMS								74,049	74,068	1866.60	86.2	0.28	85.7	34.3
NGRIP (Svenssonet al., 2013)	CFASO4	74,041	74,049	2547.16	166.7	0.13	159.4	41.4	74,055	74,059	2547.22	165.1	0.13	122.8	31.9
GRIP (This work)	IC SO4			2564.68	133.7	0.05	199.7	51.9			2564.68	133.7	0.05	156.9	40.8
NEEM (Schupbachetal., 2018)	CFASO4			2015.15	365.1	0.08	333.5	86.7			2015.15	365.1	0.08	262.0	68.1
GISP2 (Mayewskiet al., 1997)	IC SO4			2591.10	258.1	0.07	556.2	144.6			2591.10	258.1	0.07	437.0	113.6
GISP2 (Yanget al., 1996)	IC SO4			2591.60	300.0	0.07	399.6	103.9			2591.70	300.0	0.07	181.3	47.1

Ice Core	Record	T2							T3						
		Start age	End age	Depth	Bckgrd	Thinning	Deposition	Uncertainty	Start age	End age	Depth	Bckgrd	Thinning	Deposition	Uncertainty
		a b2k	a b2k	m	ppb		kg km^{-2}	kg km^{-2}	a b2k	a b2k	m	ppb		kg km^{-2}	kg km^{-2}
EDC (Svenssonet al., 2013)	FIC SO4	74,150	74,168	1079.72	147.5	0.64	49.6	19.8	74,348	74,368	1081.27	144.5	0.64	134.6	53.9
EDC (Crick et al., 2021)	ICPMS	74,146	74,172	1079.72	168.4	0.64	70.4	28.2	74,348	74,368	1081.27	204.7	0.64	124.6	49.8
EDML (Svenssonet al., 2013)	FIC SO4	74,147	74,175	1867.56	115.8	0.28	437.3	174.9	74,348	74,363	1869.51	83.7	0.28	107.2	42.9
EDML (Crick et al., 2021)	ICPMS	74,144	74,178	1867.55	101.7	0.28	427.0	170.8	74,345	74,365	1869.51	78.5	0.28	103.5	41.4
NGRIP (Svenssonet al., 2013)	CFASO4	74,154	74,161	2547.97	76.3	0.13	324.4	84.3	74,356	74,360	2550.06	57.6	0.13	60.7	15.8
GRIP (This work)	IC SO4			2565.18	90.0	0.05	442.6	115.1							
NEEM (Schupbachetal., 2018)	CFASO4			2015.48	52.3	0.08	116.3	30.2			2016.38	83.0	0.08	83.0	21.6
GISP2 (Mayewskiet al., 1997)	IC SO4			2591.64	72.3	0.07	94.8	24.6			2593.03	77.2	0.07	77.2	20.1
GISP2 (Yanget al., 1996)	IC SO4														

Ice Core	Record	T4							References		
		Start age	End age	Depth	Bckgrd	Thinning	Deposition	Uncertainty	Effective time resolution	Thinningfunction	Sulfate record and match point
		a b2k	a b2k	m	ppb		kg km^{-2}	kg km^{-2}	years		
EDC (Svenssonet al., 2013)	FIC SO4	74,479	74,491	1082.29	151.9	0.64	27.8	11.1	1.5–3	Bazin et al. (2013)	Svenssonet al. (2013)
EDC (Crick et al., 2021)	ICPMS			1083.44	152.5	0.64	24.9	10.0	1–2	Bazin et al. (2013)	Crick et al. (2021)
EDML (Svenssonet al., 2013)	FIC SO4	74,479	74,492	1870.93	89.2	0.28	237.7	95.1	1–2	Bazin et al. (2013)	Svenssonet al. (2013)
EDML (Crick et al., 2021)	ICPMS	74,474	74,495	1870.93	79.0	0.28	269.6	107.8	1–2	Bazin et al. (2013)	Crick et al. (2021)
NGRIP (Svenssonet al., 2013)	CFASO4	74,480	74,485	2551.44	41.2	0.13	72.9	18.9	1–2	Johnsenet al. (2001)	Siggaard-Andersen,PhDthesis, 2004
GRIP (This work)	IC SO4								5–10	Hvidbergetal. (1997)	This work
NEEM (Schupbachetal., 2018)	CFASO4			2016.98	78.4	0.08	102.1	26.5	10	Rasmussenet al. (2013)	Schupbach et al. (2018)
GISP2 (Mayewskiet al., 1997)	IC SO4			2593.87	68.0	0.07	171.2	44.5	50–150	Lin et al. (2022)	Mayewskiet al. (1997)
GISP2 (Yanget al., 1996)	IC SO4								1–5	Lin et al. (2022)	Yanget al. (1996)

similar linear interpolation. We then identify all of the volcanic sulfate events in Greenland and Antarctic ice cores during the 74.8–73.8 ka b2k period. If volcanic sulfate signals are identified in both Greenland and Antarctic ice cores within the annual layer counting uncertainty, we define them as bipolar volcanic events, otherwise, we classify them as unipolar events.

We applied established methods to distinguish volcanic sulfate signals from background levels and derive the volcanic sulfate content of the ice (Fischer et al., 1998; Gao et al., 2007; Karlof et al., 2005; Sigl et al., 2013; Lin et al., 2022). For each core, an ice-core flow model is applied to correct for layer thinning and to obtain volcanic sulfate deposition (Table 1; Bazin et al., 2013; Johnsen et al., 2001; Hvidberg et al., 1997; Rasmussen et al., 2013; Lin et al., 2022). The average volcanic sulfate deposition in Greenland is obtained by averaging all of the sulfate records for the same volcanic event. Due to the large distance among the Antarctic ice-core sites and the accumulation dependence of the sulfate deposition, we apply weighting factors for the two involved ice cores to obtain the average volcanic sulfate deposition following the approach of Lin et al. (2022). These weighting factors are based on the relative ratio of volcanic sulfate depositions in three synchronized (Buizert et al., 2018) Antarctic ice cores (WAIS Divide Ice Core, EDML and EDC) for the 30 largest bipolar eruptions occurred in the 60–9 ka period. The derived weighting factors for EDML and EDC are 1.15 and 1.39, respectively. The relative sulfate deposition in Greenland and Antarctica can be used to estimate the latitudinal band of the eruption site for bipolar volcanic events indicated by ice core and volcanic aerosol modelling studies (Marshall et al., 2019; Toohey et al., 2019). From previous works, the volcanic latitudinal bands for bipolar events - above 40°N, Northern Hemisphere High Latitude (NHHL), and below 40°N, Low Latitude or Southern Hemisphere (LL or SH) - can be assigned through the sulfate deposition pattern between Greenland and Antarctica (Lin et al., 2022; Abbott et al. 2021). The estimated hemispheric asymmetry ratio between Greenland and Antarctica sulfate depositions for the NHHL eruptions is above 0.69 and for the LL or SH eruptions the ratio is below 0.69. The volcanic latitudinal bands for the four Toba candidates are shown in Fig. 1, Table 2 and Table S2. From the polar volcanic sulfate depositional values, the stratospheric sulfate loading can be estimated and the associated volcanic radiative forcing can be reconstructed (Toohey and Sigl, 2017; Gao et al., 2008). We estimate the stratospheric sulfate loading by the transfer function of Gao et al. (2007). We then apply the EVA_H model to estimate the stratospheric sulfate aerosol optical depth (SAOD) from the stratospheric sulfate loading using default parameters for plume height and source location taken from historical analogue eruptions (Aubry et al., 2020). For the EVA_H model, the injection conditions - altitude and latitude parameters - for unipolar eruptions follow an Eldgjá 939 CE like eruption (12.5 km altitude, 60°N or 60°S), for the bipolar (NHHL) eruptions an Okmok 43 BCE like eruption (24 km altitude, 40°N) is applied, and for the bipolar (LL or SS) eruptions a Tambora 1815 CE like eruption (24 km altitude, 0°N) is applied. The tropopause height is defined as the average value of tropopause height from 1979 to 2016 (Thomason et al., 2018) and the eruption date of unknown volcanoes is set to 1 January consistent with previous work (Crowley and Unterman, 2013; Toohey and Sigl, 2017). To obtain the aerosol radiative forcing from SAOD we use the scaling factor of Marshall et al. (2020).

3. Results and discussion

3.1. Zooming in on the toba candidates

The ice-core volcanic signals and the reconstructed volcanic sulfate deposition in polar ice sheets for the four Toba candidates - T1, T2, T3 and T4 - are shown at Fig. S1, Table 1 and Fig. S2. For the EDC sulfate records, one volcanic sulfate peak, originally labelled as T4b by Crick et al. (2021), is repositioned at the T4 event due to a correction of that dataset (see corrigendum to Crick et al., 2021). The former T4b peak is now aligned with the T4 event in the other cores. Using the high-resolution NGRIP sulfate record and the high-resolution conductivity records of NEEM and NGRIP, it becomes evident that the Greenland T1 event is composed of two separate volcanic sulfate peaks, named T1a and T1b, that are separated by about 12 years (peak to peak) (Fig. 1 (a)). There is a 'dead' period (no volcanic sulfate signal above background) of around 6 years duration between the two events, confirming that the T1 event is composed of two distinct volcanic events (Fig. 1 (a)). Adjacent volcanic sulfate peaks can be merged in low-resolution sulfate records, but such occurrences can be identified in high-resolution dielectric profile (DEP) or electrical conductivity measurement (ECM) records of the same core. We manually separate the merged sulfate peak of the T1 events detected in the lower resolution GISP2 and NEEM sulfate records by the associated area ratio of high-resolution DEP or ECM peaks from the same cores and derive the volcanic sulfate depositions of T1a and T1b (Fig. S1 and Table 1).

As only one volcanic sulfate peak of the T1 event is detected in Antarctic ice cores (EDC and EDML), the counterpart signal in Greenland is proposed to be the T1b event. This is based on the annual layer counting, for which the period between the T2 and T1 events in Antarctica (EDML) is 84 ± 7 yrs and in Greenland (NGRIP) the period between the T2 and T1b events is 87 ± 6 yrs (Fig. 7 in

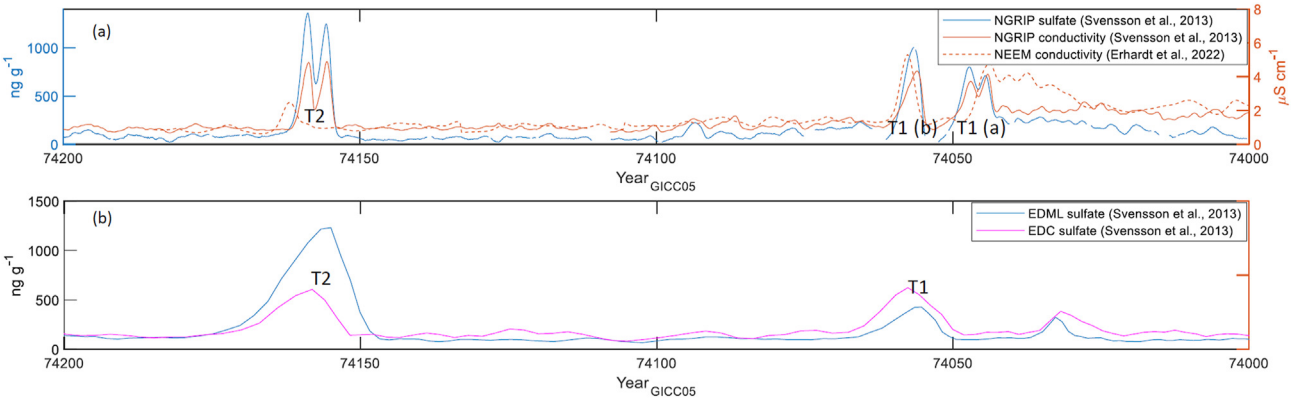

Fig. 1. Detailed information of Toba candidates - T1a, T1b and T2 on the high-resolution NGRIP sulfate record, NGRIP conductivity, NEEM conductivity, EDC sulfate and EDML sulfate records.

Table 2
Volcanic sulfate deposition of Greenland and Antarctica, stratospheric sulfate loading, latitude of eruption site and number of ice cores used to derive volcanic sulfate depositions for the Toba candidates, compared to the well-known eruptions-Pinatubo, Tambora, Salamas, Taupo and the largest unknown sulfur-rich eruption-in the past 60 ka at 45.56 ka b2k.

Eruption	Volc. Age GICC05	Volc. Duration	Antarctic volc. SO4	Greenland volc. SO4	Latitude oferuption site	Strat. Sulfate loading (SO4)	Number ofice cores		Reference
	a b2k	yrs	kg km^{-2}	kg km^{-2}		Tg	Greenland	Antarctica	
T1a	74,045	10		292.6	Unipolar	166.8	5		This study
T1b	74,057	5–16	97.6	212.7	Bipolar (NHHL)	218.9	5	4	This study
T2	74,156	7–18	290.0	244.5	Bipolar (LLor SH)	534.6	4	4	This study
T3	74,358	4–15	150.6	73.6	Bipolar (LLor SH)	224.2	3	4	This study
T4	74,484	5–12	207.2	115.4	Bipolar (LLor SH)	322.6	3	4	This study
Pinatubo	1991 CE				15°8′N, 120°21′E	25.0			Quaglia et al. (2023)
Tambora	1815 CE	2–3	45.8	39.7	8°15′S, 118°E	85.5	1	2	Sigl et al. (2015)
Salamas	1258 CE	2.4–3.8	90.4	73.2	8°42′S, 116°24′E	163.6	1	2	Sigl et al. (2015)
Taupo	24.46 ka b2k	3–7	192.8	189.5	Bipolar (LLor SH)	382.3	2	3	Lin et al. (2022)
Unknown[a]	45.56 ka b2k	6–14	172.7	652.6	Bipolar (NHHL)	544.7	3	3	Lin et al. (2022)

[a] The largesteruption inthe period (60–0 ka).

Svensson et al. (2013)). As the annual layer counting between the T1a and T1b events in Greenland (NGRIP) is 12 years, it is most likely that T1b is the bipolar volcanic event. However, as exact annual layer counting is challenging at this depth, we can not firmly rule out that the T1a event is related to the T1 event in Antarctica.

3.2. Tracing the toba eruption

In the following, we combine multiple lines of evidence to propose the most likely candidate for the Toba event from the four proposed eruptions. As the stratigraphic setting of the Toba eruption is right at the cooling transition leading to GS-20 in several marine records (Fig. S6 in Deplazes et al., 2013, Fig. 3 in Schulz et al., 1998), we propose that the Toba eruption has to be found among the T1-T4. From the Greenland and Antarctic sulfate deposition derived in this study, we have estimated the sulfur emission strength of the individual eruptions. The ratio of volcanic sulfate deposition in Greenland and Antarctica allows us to predict the latitudinal band of the eruption site (NHHL, and LL or SH). In addition, the ice-core sulfur isotopic composition of the Toba candidates indicates whether the eruption plume reached the stratosphere and provides an indication of the minimum height of the eruption plume (Savarino et al., 2003; Crick et al., 2021).

As discussed in section 3.1, the T1 event is associated with two separate events (T1a and T1b), of which the T1b event is most likely to be related to the Antarctic T1 event, and the T1a event is proposed to be a Northern Hemisphere extratropical eruption with no imprint in Antarctic ice cores (NHHL). Despite the lack of certainty regarding which of the two Greenland events is bipolar, the rather low T1 Antarctic sulfate deposition compared to the T1a or T1b sulfate depositions in Greenland strongly suggests that both events are related to eruptions that occurred above 40°N (Fig. 2 (a) and Fig. 2 (b)). The clear Northern Hemispheric dominance of the T1a and the T1b events thus makes both of them unlikely to originate from the Toba eruption.

The T2 event has by far the largest stratospheric sulfate loading (534.57 ± 96.3 Tg) of the four Toba candidates (Fig. 2 (c)). It is also stronger than any bipolar eruption signal identified from ice cores

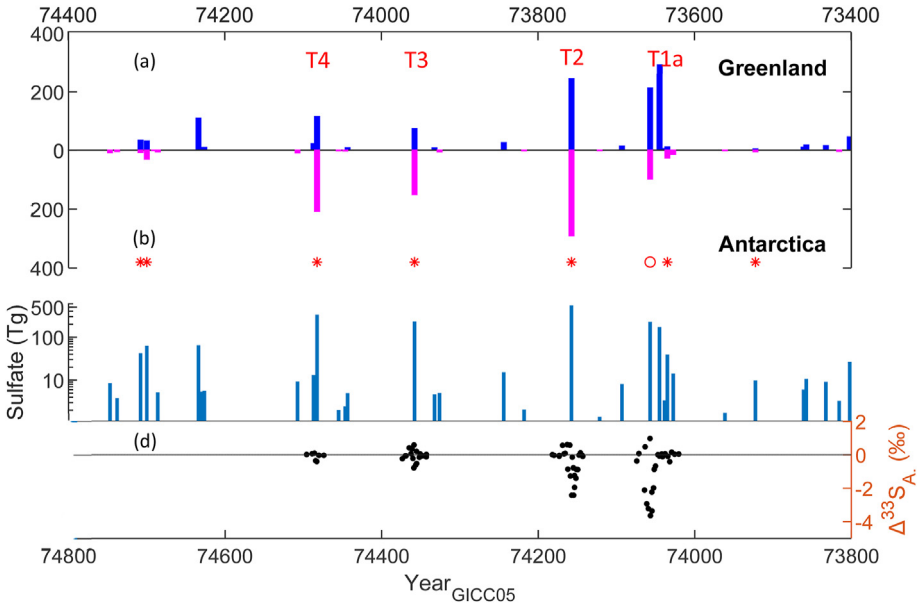

Fig. 2. (a) Ice-core derived volcanic sulfate depositions in Greenland and Antarctica. (b) '*' denotes that the predicted latitudinal band of eruption site occurred below 40°N (LL or SH) and 'o' denotes ones occurred above 40°N (NHHL) for bipolar volcanic eruptions. (c) The stratospheric sulfate loading derived from Greenland and Antarctic volcanic sulfate depositions list. (d) The sulfur isotope $\Delta^{33}S$ measured by Crick et al. (2021) from Antarctic ice cores for the Toba candidates.

in the 60–9 ka period (Lin et al., 2022). Relative to the stratospheric sulfate loading for the T2 event derived by Crick et al. (2021), our value is 24% lower, mainly because five more sulfate records from Greenland and Antarctica are included in this study. The even distribution of sulfate deposition between the two hemispheres (Greenland versus Antarctica) suggests the event occurred at low latitudes (Fig. 2 (b) and Table 2). The Antarctic sulfur isotopic composition shows that the eruption plume reached the stratosphere and that the top of plume height may have exceeded 45 km (Crick et al., 2021). Therefore, the T2 event fulfills all criteria for being related to the Toba eruption.

The T3 event has a stratospheric sulfate loading of 224.21 ± 15.7 Tg, about 9 times that of the Pinatubo 1991 CE eruption and 2.6 times that of the Tambora 1815 CE eruption, but it is weaker than those of the T2 and T4 events (Table 2). The hemispheric sulfate distribution of the T3 event suggests that the event occurred below 40°N. The Antarctic sulfur isotopic signals of the T3 event suggests that the eruption plume reached the stratosphere, but the top of the plume height is lower than those of the T2 and T1 events (Fig. 2 (d) (Crick et al., 2021). Overall, this implies that the T3 event was not of a sufficient magnitude to be associated with the Toba eruption.

The sulfate emission strength of the T4 event is larger than that of the T3 event but smaller than that of the T2 event. The relative hemispheric sulfate deposition in Greenland and Antarctica implies that the eruption site was most likely in the tropics or the Southern Hemisphere. The magnitude of the Antarctic sulfur isotopic signals suggests that the eruption site was likely located in the extratropical SH area (Crick et al., 2021) (Fig. 2 (d)). For this reason, the T4 event is unlikely to be associated with the Toba eruption.

The positive relationship between the stratospheric sulfate loading quantified from ice cores and the volcanic explosivity index (VEI) of the same event has been observed from well known historical eruptions. If the T2 event is the Toba eruption, the T1a and T1b events are related to the NH extratropical eruptions, and the eruption plume of the T4 is mostly constrained to the troposphere, the T3 event appears the most likely candidate of another unknown large sulfur-rich eruption. A recent (U–Th)/He dating age of the Los Chocoyos (LC) eruption of the Atitlán volcano, that occurred in present-day Guatemala, is 75 ± 2 ka (Cisneros de Leon et al., 2021), that is not consistent with previously dated age of 84 ka BP (Drexler et al., 1980). As no tephra of the LC eruption has been identified either in Greenland or Antarctic ice cores, we could not assign the LC eruption to one of the T1-T4.

The stratospheric sulfate loading of the T2 event is estimated to be 1.4 times that of the Oruanui, Taupo (New Zealand, VEI-8) supereruption dated 25.37 ± 0.25 ka in the annual-layer counted WD2014 chronology from Antarctica (Sigl et al., 2016), which was identified in an ice core through cryptotephra fingerprinting (Dunbar et al., 2017) and its sulfur emission strength is ranked fourth in the ice-core volcano list of the last 60 ka (Lin et al., 2022). In terms of stratospheric sulfate loading, the T2 eruption is comparable to the largest eruption identified in the 60–9 ka period, that occurred at 45.56 ka b2k. However, as the 45.56 ka b2k eruption most likely occurred in the extratropical NH (Lin et al., 2022), the T2 event is suspected to have the strongest climatic impact of the two based on the assumption that the sulfate aerosol burden time of tropical eruptions is longer than that of extratropical NH eruptions (Marshall et al., 2019). The climatic impact of more recent large bipolar eruptions - Samalas 1257 CE, Tambora 1815 CE and Pinatubo 1991 CE – was a lowering of global mean temperature of 0.5–1.2 °C, lasting for several years (Raible et al., 2016; Parker et al., 1996; Guillet et al., 2017). The stratospheric sulfate loading of the T2 event is 3 times that of Samalas, 6 times that of Tambora and 20 times that of Pinatubo (Table 2), indicating that a more extreme cooling could have followed the Toba eruption. Compared to the wider range of the sulfur emission strength estimated from petrological evidence (10–360 times that of the Pinatubo eruption; Chesner and Luhr, 2010; Scaillet et al., 1998; Oppenheimer, 2002), we estimate a stratospheric sulfate loading of 535 ± 96 Tg derived from ice cores for the Toba eruption, that is 20 times that of the Pinatubo eruption. This estimate supports the relatively low sulfur emission scenarios in model simulations for the Toba eruption (Black et al., 2021; Osipov et al., 2020; Robock et al., 2009; Timmreck et al., 2012). Black et al. (2021) found that 300 Tg of stratospheric sulfate loading led to a 2.3 ± 0.4 °C lowering of the

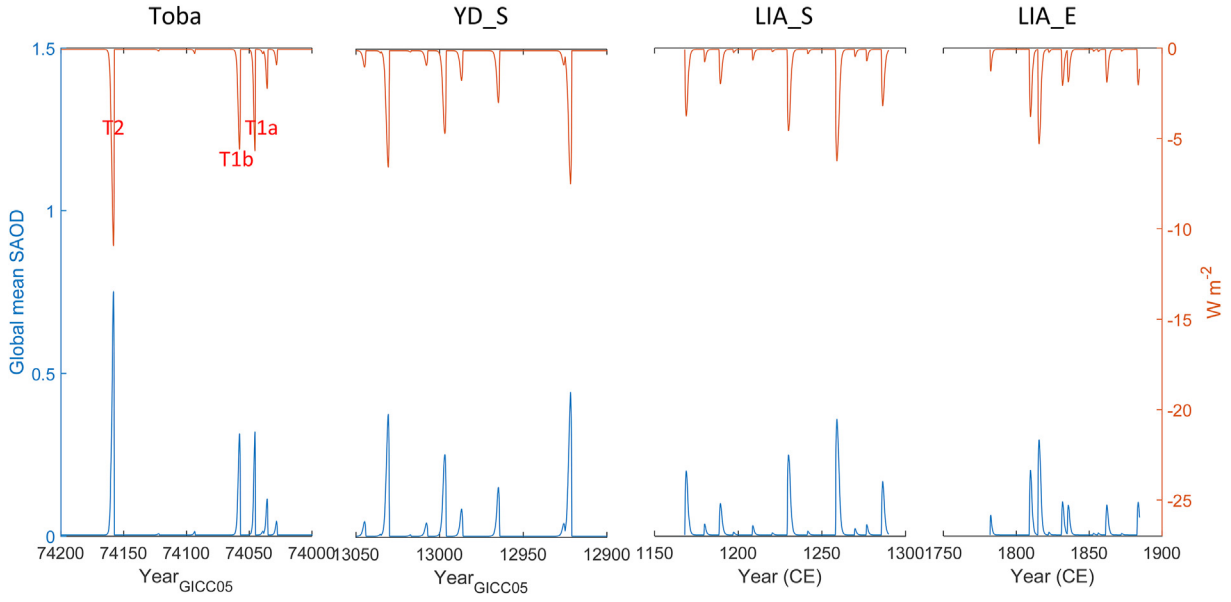

Fig. 3. Comparison of monthly global mean SAOD and estimated volcanic radiative forcing for the enhanced volcanic period of 74,158–74045 (a b2k) including the Toba candidates (T2, T1a and T1b) to the three well investigated periods – at the onset of Youngers Dryas (13,030–12921 a b2k) (Abbott et al.) (labelled as YD_S), the Little Ice Age (1171–1286 CE) (labelled as LIA_S), and Little Ice Age (1783–1890 CE) (labelled as LIA_E) (Toohey and Sigl, 2017).

annual mean global surface temperature.

3.3. Volcanic forcing at the GS-20 onset and comparison with other periods of enhanced volcanic activity

Thirty-five volcanic eruptions have been identified in polar ice cores in the investigated period of 74.8–73.8 ka b2k (Table S2). Among them, eight volcanic sulfate signals are identified as bipolar volcanic eruptions with stratospheric sulfate loading above 10 Tg. Fourteen volcanic sulfate signals are identified only in Greenland ice cores and 13 volcanic sulfate signals are identified only in Antarctica. The global mean and the 30°- 90°N mean of the SAOD as well as the radiative forcing are reconstructed over this period (Table S3).

We define the 'Toba' period at the end of the cooling transition leading to GS-20 as 74,158–74,045 a b2k, and we compare this interval to younger periods of enhanced volcanic activity that are associated with long-term cooling and ice growth. The 'Toba' interval contains three major eruptions (T1a, T1b and T2). The three periods selected for comparison are located at the onset of Younger Dryas event (YD_S, 13,030–12,921 a b2k), the start of the Little Ice Age (LIA_S, 1171–1286 CE) and the end of the Little Ice Age (LIA_E, 1783–1890 CE), following the approach of Abbott et al. (2012) (Fig. 3 and Table S3). For these three volcanically enhanced periods, we applied the same approach as Lin et al. (2022) to estimate the stratospheric sulfate loading and to reconstruct the volcanic radiative forcing from the published Greenland and Antarctic volcanic sulfate deposition records (Abbott et al.; Sigl et al., 2013; Table S3). The results presented here differ from those of Abbott et al. (2012) due to the different weighting of the Greenland volcanic sulfate deposition applied to derive the stratospheric sulfate loading for extratropical NH bipolar eruptions. Here we assume that volcanic sulfate transport and deposition over Greenland are influenced by the polar vortex transport patterns (Gao et al., 2007). Using this approach, the centennial cumulative stratospheric aerosol loading for the volcanically active periods - YD_S, LIA_S and LIA_E - are respectively 40%, 8% and 7% lower than those estimated by Abbott et al. (2012) and Toohey and Sigl (2017). The centennial cumulative stratospheric aerosol loading, the mean global SAOD and the mean SAOD at 30–90°N of the 'Toba' period is much stronger than those of the other three periods (Table S4). Due to the distinct volcanic cluster and the extreme volcanic forcing at the onset of the GS-20, we discuss the possibility of an amplified and prolonged cooling beyond the stratospheric sulfate aerosol burden induced cooling in the following.

3.4. Potential longer-term climatic impact of the T1 and T2 eruptions

The behaviour of the ice-core water isotopic proxies - $\delta^{18}O$ and deuterium excess (d-excess) - at the T1 and T2 events may provide clues about the climatic impact of those eruptions in both hemispheres.

Using a stack of four $\delta^{18}O$ records from the NGRIP (NGRIP members, 2004), GISP2 (Grootes and Stuiver, 1997), NEEM (Gkinis et al., 2021) and GRIP (Johnsen et al., 2001) cores (Fig. S3 (d-g)), we observe an accelerated cooling transition (a steepening of the isotopic trend) right after the T2 event for a 110 yr period prior to GS-20 (Fig. 4 (c)). The interpretation of this increased cooling trend could be that the very large volcanic eruption induced a cooling of the atmosphere and the upper mixed ocean, leading to increased sea-ice cover in the North Atlantic. This hypothesis is supported by the NGRIP and NEEM d-excess records (Svensson et al., 2013; Gkinis et al., 2021), a proxy for the temperature of the Greenland vapor source areas (Steffensen et al., 2008). Both the individual and the stacked d-excess records show an abrupt shift right at the T2 eruption (Fig. 4 (a) and Fig. S3 (b, c)), suggesting a southern shift of the water vapor source resulting from the extended sea ice cover.

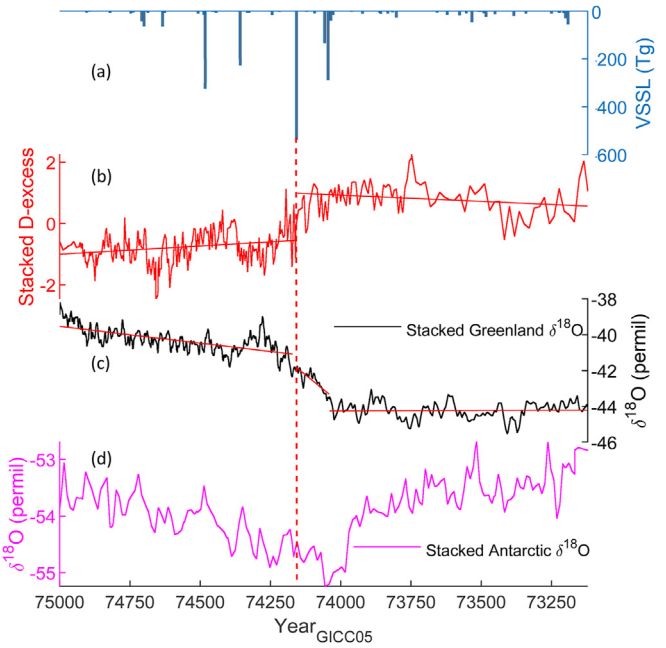

Fig. 4. Abrupt climate variability at the termination of GI-20. (a), The volcanic stratospheric sulfate loading (VSSL). (b), The stacked normalized NGRIP and NEEM deuterium excess records. Two disconnected linear fits (intervals: >74,156, 74,156–73121) represent in red color. (c), The stacked $\delta^{18}O$ records of NGRIP, NEEM, GISP2 and GRIP ice cores in Greenland. Three disconnected linear fits (intervals: >74,156, 74,156–74041, 74,041–73121) represent in red color. (d), The stacked $\delta^{18}O$ records of EDC, EDML and DF ice cores in Antarctica.

The $\delta^{18}O$ records of the EDML (EPICA community members, 2006), EDC (EPICA community members, 2004), and Dome F (Kawamura et al., 2007) ice cores in Antarctica do not indicate any extended cooling following the T2 eruption (Fig. 4 (d), Fig. S3 (i) and Fig. S3 (h)), indicating the uneven regional temperature followed the T2 eruption in Antarctica. An interpretation of this behaviour is that the Greenland and Antarctic temperature proxies follow a 'bipolar seesaw' pattern and that the NH extended sea ice cover triggered by the T2 eruption may weaken the Atlantic meridional overturning circulation and induce a delayed warming in Antarctica that is most likely perturbed by the strong T1 eruption. This mechanism is in agreement with the interpretation of Stocker and Johnsen (2003) and with model simulation results (Robock et al., 2009; Timmreck et al., 2012).

4. Conclusions

We pinpoint the Toba eruption from ice-core records by combining information from synchronized high-resolution ECM and DEP records, the sulfur isotopic signals, the sulfur emission strength and the estimated latitudinal band of eruption sites. From the previously identified Toba candidates - T1, T2, T3 and T4, we propose the T2 event to be related to the Toba eruption, because the T2 event has a clear tropical origin and its sulfur emission strength is larger than the other Toba candidates and any other volcanic events identified in ice core records between 60 and 9 kyr. Previous studies of the Toba eruption using a single ice-core, mineral chemistry or experimental petrology have produced a wide range of estimates for sulfur emitting, from 105 Tg to 9900 Tg. We estimate that the stratospheric sulfate loading of the proposed Toba

eruption is 535 ± 96 Tg. Since this is the largest recorded signal within the radiometric age limits of the Toba eruption, our reconstruction provides an upper bound of similarly to 20 times the injection of the Pinatubo, which is used as input for many climate model experiments for this eruption, e.g. 33 to 900 times the Pinatubo injection (Robock et al., 2009).

Further support for this proposition could be gained if tephra from the Toba eruption was found in direct association with the T2 chemical signal, however, tephra investigations of NGRIP for all the Toba candidates did not yield any glass shards (Abbott et al., 2012).

Within one thousand years of volcanic reconstruction at the cooling transition to Greenland Stadial 20, thirty-five volcanic eruptions have been identified. Towards the end of this period, three major eruptions -T1a, T1b and T2 — show an extreme volcanic forcing that is unparalleled in later periods such as at the onset of the Younger Dryas period and the Little Ice Age. Following the proposed Toba eruption, an abrupt shift is observed in Greenland temperature proxies, suggesting that the climatic forcing of the Toba eruption has accelerated the cooling transition leading to the extremely cold GS-20 period, possibly due to sea-ice extension in the North Atlantic. The reconstructed volcanic forcing can be incorporated in model simulations in order to investigate mechanisms of abrupt climate change, and to quantify the global climatic impact of the Toba eruption and the volcanic cluster occurring at the cooling transition leading to GS-20.

Author contributions

All the authors contributed to this manuscript. JL wrote the paper draft with AS. JL analysed the data and created the figures. AS, JL, JP, RM, MS were involved in obtaining the applied datasets. All authors commented on the paper.

Declaration of competing interest

The authors declare that they have no known competing financial interests or personal relationships that could have appeared to influence the work reported in this paper.

Data availability

No data was used for the research described in the article.

Acknowledgements

Jiamei Lin acknowledges support from the China Scholarship Council. PA and MSi received funding from the European Research Council under the European Union's Horizon 2020 research and innovation programme (grant agreement no. 820047).

Appendix A. Supplementary data

Supplementary data to this article can be found online at https://doi.org/10.1016/j.quascirev.2023.108162.

References

Abbott, P.M., Davies, S.M., Steffensen, J.P., Pearce, N.J.G., Bigler, M., Johnsen, S.J., Seierstad, I.K., Svensson, A., Wastegård, S., 2012. A detailed framework of marine isotope stage 4 and 5 volcanic events recorded in two Greenland ice-cores. Quat. Sci. Rev. 36, 59–77.

Abbott, P.M., Niemeier, U., Timmreck, C., Riede, F., McConnell, J.R., Severi, M., Fischer, H., Svensson, A., Toohey, M., Reinig, F., Sigl, M., 2021. Volcanic climate forcing preceding the inception of the Younger Dryas: implications for tracing the Laacher See eruption. Quat. Sci. Rev. 274. https://doi.org/10.1016/j.quascirev.2021.107260.

Ambrose, S.H., 1998. Late Pleistocene human population bottlenecks, volcanic winter, and differentiation of modern humans. J. Hum. Evol. 34, 623–651. https://doi.org/10.1006/jhev.1998.0219.

Aubry, T.J., Toohey, M., Marshall, L., Schmidt, A., Jellinek, A.M., 2020. A new volcanic stratospheric sulfate aerosol forcing emulator (EVA_H): comparison with interactive stratospheric aerosol models. J. Geophys. Res. Atmos. 125. https://doi.org/10.1029/2019jd031303.

Baldini, J.U.L., Brown, R.J., McElwaine, J.N., 2015. Was millennial scale climate change during the Last Glacial triggered by explosive volcanism? Sci. Rep. 5. https://doi.org/10.1038/srep17442.

Bazin, L., Landais, A., Lemieux-Dudon, B., Kele, H.T.M., Veres, D., Parrenin, F., Martinerie, P., Ritz, C., Capron, E., Lipenkov, V., Loutre, M.F., Raynaud, D., Vinther, B., Svensson, A., Rasmussen, S.O., Severi, M., Blunier, T., Leuenberger, M., Fischer, H., Masson-Delmotte, V., Chappellaz, J., Wolff, E., 2013. An optimized multi-proxy, multi-site Antarctic ice and gas orbital chronology (AICC2012): 120-800 ka. Clim. Past 9, 1715–1731. https://doi.org/10.5194/cp-9-1715-2013.

Black, B.A., Lamarque, J.F., Marsh, D.R., Schmidt, A., Bardeen, C.G., 2021. Global climate disruption and regional climate shelters after the Toba supereruption. Proc. Natl. Acad. Sci. U. S. A 118. https://doi.org/10.1073/pnas.2013046118.

Brenna, H., Kutterolf, S., Mills, M.J., Kruger, K., 2020. The potential impacts of a sulfur- and halogen-rich supereruption such as Los Chocoyos on the atmosphere and climate. Atmos. Chem. Phys. 20, 6521–6539. https://doi.org/10.5194/acp-20-6521-2020.

Buhring, C., Sarnthein, M., 2000. Leg 184 Shipboard Sci, P.: Toba ash layers in the South China Sea: evidence of contrasting wind directions during eruption ca. 74 ka. Geology 28, 275–278. https://doi.org/10.1130/0091-7613(2000)028<0275:Talits>2.3.Co;2.

Buizert, C., Sigl, M., Severi, M., Markle, B.R., Wettstein, J.J., McConnell, J.R., Pedro, J.B., Sodemann, H., Goto-Azuma, K., Kawamura, K., Fujita, S., Motoyama, H., Hirabayashi, M., Uemura, R., Stenni, B., Parrenin, F., He, F., Fudge, T.J., Steig, E.J., 2018. Abrupt ice-age shifts in southern westerly winds and Antarctic climate forced from the north. Nature 563, 681. https://doi.org/10.1038/s41586-018-0727-5.

Chesner, C.A., Luhr, J.F., 2010. A melt inclusion study of the Toba Tuffs, Sumatra, Indonesia. J. Volcanol. Geoth. Res. 197, 259–278. https://doi.org/10.1016/j.jvolgeores.2010.06.001.

Chesner, C.A., Rose, W.I., Deino, A., Drake, R., Westgate, J.A., 1991. Eruptive history of Earth's largest Quaternary caldera (Toba, Indonesia) clarified. Geology 19, 200–203. https://doi.org/10.1130/0091-7613(1991)019<0200:Ehoesl>2.3.Co;2.

Cisneros de Leon, A., Schindlbeck-Belo, J.C., Kutterolf, S., Danisik, M., Schmitt, A.K., Freundt, A., Perez, W., Harvey, J.C., Wang, K.L., Lee, H.Y., 2021. A history of violence: magma incubation, timing and tephra distribution of the Los Chocoyos supereruption (Atitlan Caldera, Guatemala). J. Quat. Sci. 36, 169–179. https://doi.org/10.1002/jqs.3265.

Clarkson, C., Harris, C., Li, B., Neudorf, C.M., Roberts, R.G., Lane, C., Norman, K., Pal, J., Jones, S., Shipton, C., Koshy, J., Gupta, M.C., Mishra, D.P., Dubey, A.K., Boivin, N., Petraglia, M., 2020. Human occupation of northern India spans the Toba supereruption similar to 74,000 years ago. Nat. Commun. 11. https://doi.org/10.1038/s41467-020-14668-4.

Crick, L., Burke, A., Hutchison, W., Kohno, M., Moore, K.A., Savarino, J., Doyle, E.A., Mahony, S., Kipfstuhl, S., Rae, J.W.B., Steele, R.C.J., Sparks, R.S.J., Wolff, E.W., 2021. New insights into the similar to 74 ka Toba eruption from sulfur isotopes of polar ice cores. Clim. Past 17, 2119–2137. https://doi.org/10.5194/cp-17-2119-2021.

Crowley, T.J., Unterman, M.B., 2013. Technical details concerning development of a 1200 yr proxy index for global volcanism. Earth Syst. Sci. Data 5, 187–197. https://doi.org/10.5194/essd-5-187-2013.

Deplazes, G., Luckge, A., Peterson, L.C., Timmermann, A., Hamann, Y., Hughen, K.A., Rohl, U., Laj, C., Cane, M.A., Sigman, D.M., Haug, G.H., 2013. Links between tropical rainfall and North Atlantic climate during the last glacial period. Nat. Geosci. 6, 213–217. https://doi.org/10.1038/ngeo1712.

Dunbar, N.W., Iverson, N.A., Van Eaton, A.R., Sigl, M., Alloway, B.V., Kurbatov, A.V., Mastin, L.G., McConnell, J.R., Wilson, C.J.N., 2017. New Zealand supereruption provides time marker for the Last Glacial Maximum in Antarctica. Sci. Rep. 7. https://doi.org/10.1038/s41598-017-11758-0.

Drexler, J.W., Rose, W.I., Sparks, R.S.J., Ledbetter, M.T., 1980. The Los Chocoyos Ash, Guatemala: a major stratigraphic marker in middle America and in three ocean basins. Quat. Res. (Tokyo) 13, 327–345. https://doi.org/10.1016/0033-5894(80)90061-7.

EPICA community members, 2004. Eight glacial cycles from an Antarctic ice core. Nature 429, 623–628.

EPICA community members, 2006. One-to-one coupling of glacial climate variability in Greeland and Antartctica. Nature 444, 195–198.

Fischer, H., Wagenbach, D., Kipfstuhl, J., 1998. Sulfate and nitrate firn concentrations on the Greenland ice sheet - 2. Temporal anthropogenic deposition changes. J. Geophys. Res. Atmos. 103, 21935–21942. https://doi.org/10.1029/98jd01886.

Gao, C.C., Robock, A., Ammann, C., 2008. Volcanic forcing of climate over the past 1500 years: an improved ice core-based index for climate models. J. Geophys. Res. Atmos. 113. https://doi.org/10.1029/2008jd010239.

Gao, C.H., Oman, L., Robock, A., Stenchikov, G.L., 2007. Atmospheric volcanic loading derived from bipolar ice cores: accounting for the spatial distribution of volcanic deposition. J. Geophys. Res. Atmos. 112. https://doi.org/10.1029/2006jd007461.

Ge, Y., Gao, X., 2020. Understanding the overestimated impact of the Toba volcanic super-eruption on global environments and ancient hominins. Quat. Int. 559,

24–33. https://doi.org/10.1016/j.quaint.2020.06.021.
Gkinis, V., Vinther, B.M., Popp, T.J., Quistgaard, T., Faber, A.K., Holme, C.T., Jensen, C.M., Lanzky, M., Lutt, A.M., Mandrakis, V., Orum, N.O., Pedersen, A.S., Vaxevani, N., Weng, Y.B., Capron, E., Dahl-Jensen, D., Horhold, M., Jones, T.R., Jouzel, J., Landais, A., Masson-Delmotte, V., Oerter, H., Rasmussen, S.O., Steen-Larsen, H.C., Steffensen, J.P., Sveinbjornsdottir, A.E., Svensson, A., Vaughn, B., White, J.W.C., 2021. A 120,000-year long climate record from a NW-Greenland deep ice core at ultra-high resolution. Sci. Data 8. https://doi.org/10.1038/s41597-021-00916-9.
Grootes, P.M., Stuiver, M., 1997. Oxygen 18/16 variability in Greenland snow and ice with 10^{-3} - 10^{5}-year time resolution. J. Geophys. Res. 102, 26455–26470.
Guillet, S., Corona, C., Stoffel, M., Khodri, M., Lavigne, F., Ortega, P., Eckert, N., Sielenou, P.D., Daux, V., Churakova, O.V., Davi, N., Edouard, J.L., Zhang, Y., Luckman, B.H., Myglan, V.S., Guiot, J., Beniston, M., Masson-Delmotte, V., Oppenheimer, C., 2017. Climate response to the Samalas volcanic eruption in 1257 revealed by proxy records. Nat. Geosci. 10, 123. https://doi.org/10.1038/ngeo2875.
Huang, C.Y., Zhao, M.X., Wang, C.C., Wei, G.J., 2001. Cooling of the South China Sea by the Toba eruption and correlation with other climate proxies similar to 71,000 years ago. Geophys. Res. Lett. 28, 3915–3918. https://doi.org/10.1029/2000gl006113.
Hvidberg, C.S., DahlJensen, D., Waddington, E.D., 1997. Ice flow between the Greenland ice core Project and Greenland ice sheet Project 2 boreholes in central Greenland. Journal of Geophysical Research-Oceans 102, 26851–26859. https://doi.org/10.1029/97jc00268.
Jackson, L.J., Stone, J.R., Cohen, A.S., Yost, C.L., 2015. High-resolution paleoecological records from Lake Malawi show no significant cooling associated with the Mount Toba supereruption at ca. 75 ka. Geology 43, 823–826. https://doi.org/10.1130/g36917.1.
Johnsen, S.J., DahlJensen, D., Gundestrup, N., Steffensen, J.P., Clausen, H.B., Miller, H., Masson-Delmotte, V., Sveinbjornsdottir, A.E., White, J., 2001. Oxygen isotope and palaeotemperature records from six Greenland ice-core stations: camp Century, Dye-3, GRIP, GISP2, Renland and NorthGRIP. J. Quat. Sci. 16, 299–307. https://doi.org/10.1002/jqs.622.
Karlof, L., Oigard, T.A., Godtliebsen, F., Kaczmarska, M., Fischer, H., 2005. Statistical techniques to select detection thresholds for peak signals in ice-core data. J. Glaciol. 51, 655–662. https://doi.org/10.3189/172756505781829115.
Kawamura, K., Parrenin, F., Lisiecki, L., Uemura, R., Vimeux, F., Severinghaus, J.P., Hutterli, M.A., Nakazawa, T., Aoki, S., Jouzel, J., Raymo, M.E., Matsumoto, K., Nakata, H., Motoyama, H., Fujita, S., Goto-Azuma, K., Fujii, Y., Watanabe, O., 2007. Northern Hemisphere forcing of climatic cycles in Antarctica over the past 360,000 years. Nature 448, 912–914. https://doi.org/10.1038/nature06015.
Lane, C.S., Chorn, B.T., Johnson, T.C., 2013. Ash from the Toba supereruption in Lake Malawi shows no volcanic winter in East Africa at 75 ka. Proc. Natl. Acad. Sci. U. S. A 110, 8025–8029. https://doi.org/10.1073/pnas.1301474110.
Lin, J.M., Svensson, A., Hvidberg, C.S., Lohmann, J., Kristiansen, S., Dahl-Jensen, D., Steffensen, J.P., Rasmussen, S.O., Cook, E., Kjaeer, H.A., Vinther, B.M., Fischer, H., Stocker, T., Sigl, M., Bigler, M., Severi, M., Traversi, R., Mulvaney, R., 2022. Magnitude, frequency and climate forcing of global volcanism during the last glacial period as seen in Greenland and Antarctic ice cores (60-9 ka). Clim. Past 18, 485–506. https://doi.org/10.5194/cp-18-485-2022.
Liu, Z.F., Colin, C., Trentesaux, A., 2006. Major element geochemistry of glass shards and minerals of the Youngest Toba Tephra in the southwestern South China Sea. J. Asian Earth Sci. 27, 99–107. https://doi.org/10.1016/j.jseaes.2005.02.003.
Lohmann, J., Svensson, A., 2022. Ice core evidence for major volcanic eruptions at the onset of Dansgaard–Oeschger warming events. Clim. Past 18, 2021–2043. https://doi.org/10.5194/cp-18-2021-2022.
Mark, D.F., Petraglia, M., Smith, V.C., Morgan, L.E., Barfod, D.N., Ellis, B.S., Pearce, N.J., Pal, J.N., Korisettar, R., 2014. A high-precision Ar-40/Ar-39 age for the Young Toba Tuff and dating of ultra-distal tephra: forcing of Quaternary climate and implications for hominin occupation of India. Quat. Geochronol. 21, 90–103. https://doi.org/10.1016/j.quageo.2012.12.004.
Mark, D.F., Renne, P.R., Dymock, R.C., Smith, V.C., Simon, J.I., Morgan, L.E., Staff, R.A., Ellis, B.S., Pearce, N.J.G., 2017. High-precision 40Ar/39Ar dating of pleistocene tuffs and temporal anchoring of the Matuyama-Brunhes boundary. Quat. Geochronol. 39, 1–23. https://doi.org/10.1016/j.quageo.2017.01.002.
Marshall, L., Johnson, J.S., Mann, G.W., Lee, L., Dhomse, S.S., Regayre, L., Yoshioka, M., Carslaw, K.S., Schmidt, A., 2019. Exploring how eruption source parameters affect volcanic radiative forcing using statistical emulation. J. Geophys. Res. Atmos. 124, 964–985. https://doi.org/10.1029/2018jd028675.
Marshall, L.R., Smith, C.J., Forster, P.M., Aubry, T.J., Andrews, T., Schmidt, A., 2020. Large variations in volcanic aerosol forcing efficiency due to eruption source parameters and rapid adjustments. Geophys. Res. Lett. 47. https://doi.org/10.1029/2020gl090241.
Mayewski, P.A., Meeker, L.D., Twickler, M.S., Whitlow, S., Yang, Q.Z., Lyons, W.B., Prentice, M., 1997. Major features and forcing of high-latitude northern hemisphere atmospheric circulation using a 110,000-year-long glaciochemical series. Journal of Geophysical Research-Oceans 102, 26345–26366. https://doi.org/10.1029/96jc03365.
McConnell, J.R., Burke, A., Dunbar, N.W., Kohler, P., Thomas, J.L., Arienzo, M.M., Chellman, N.J., Maselli, O.J., Sigl, M., Adkins, J.F., Baggenstos, D., Burkhart, J.F., Brook, E.J., Buizert, C., Cole-Dai, J., Fudge, T.J., Knorr, G., Graf, H.F., Grieman, M.M., Iverson, N., McGwire, K.C., Mulvaney, R., Paris, G., Rhodes, R.H., Saltzman, E.S., Severinghaus, J.P., Steffensen, J.P., Taylor, K.C., Winckler, G., 2017. Synchronous volcanic eruptions and abrupt climate change similar to 17.7 ka plausibly linked by stratospheric ozone depletion. Proc. Natl. Acad. Sci. U. S. A 114, 10035–10040. https://doi.org/10.1073/pnas.1705595114.
McConnell, J.R., Sigl, M., Plunkett, G., Burke, A., Kim, W.M., Raible, C.C., Wilson, A.I., Manning, J.G., Ludlow, F., Chellman, N.J., Innes, H.M., Yang, Z., Larsen, J.F., Schaefer, J.R., Kipfstuhl, S., Mojtabavi, S., Wilhelms, F., Opel, T., Meyer, H., Steffensen, J.P., 2020. Extreme climate after massive eruption of Alaska's Okmok volcano in 43 BCE and effects on the late Roman Republic and Ptolemaic Kingdom. Proc. Natl. Acad. Sci. U. S. A 117, 15443–15449. https://doi.org/10.1073/pnas.2002722117.
Miller, G.H., Geirsdottir, A., Zhong, Y.F., Larsen, D.J., Otto-Bliesner, B.L., Holland, M.M., Bailey, D.A., Refsnider, K.A., Lehman, S.J., Southon, J.R., Anderson, C., Bjornsson, H., Thordarson, T., 2012. Abrupt onset of the Little Ice Age triggered by volcanism and sustained by sea-ice/ocean feedbacks. Geophys. Res. Lett. 39. https://doi.org/10.1029/2011gl050168.
Oppenheimer, C., 2002. Limited global change due to the largest known Quaternary eruption, Toba approximate to 74 kyr BP? Quat. Sci. Rev. 21, 1593–1609. https://doi.org/10.1016/s0277-3791(01)00154-8.
Osipov, S., Stenchikov, G., Tsigaridis, K., LeGrande, A.N., Bauer, S.E., 2020. The role of the SO2 radiative effect in sustaining the volcanic winter and soothing the Toba impact on climate. J. Geophys. Res. Atmos. 125. https://doi.org/10.1029/2019jd031726.
Paine, A.R., Wadsworth, F.B., Baldini, J.U.L., 2021. Supereruption doublet at a climate transition. Communications Earth & Environment 2. https://doi.org/10.1038/s43247-021-00293-6, 219.
Parker, D.E., Wilson, H., Jones, P.D., Christy, J.R., Folland, C.K., 1996. The impact of Mount Pinatubo on world-wide temperatures. Int. J. Climatol. 16, 487–497. https://doi.org/10.1002/(sici)1097-0088(199605)16:5<487::Aid-joc39>3.0.Co;2-j.
Pausata, F.S.R., Chafik, L., Caballero, R., Battisti, D.S., 2015. Impacts of high-latitude volcanic eruptions on ENSO and AMOC. Proc. Natl. Acad. Sci. U. S. A 112, 13784–13788. https://doi.org/10.1073/pnas.1509153112.
Pearce, N.J.G., Westgate, J.A., Gatti, E., Pattan, J.N., Parthiban, G., Achyuthan, H., 2014. Individual glass shard trace element analyses confirm that all known Toba tephra reported from India is from the c. 75-ka Youngest Toba eruption. J. Quat. Sci. 29, 729–734. https://doi.org/10.1002/jqs.2741.
Quaglia, I., Timmreck, C., Niemeier, U., Visioni, D., Pitari, G., Brodowsky, C., Brühl, C., Dhomse, S.S., Franke, H., Laakso, A., Mann, G.W., Rozanov, E., Sukhodolov, T., 2023. Interactive stratospheric aerosol models' response to different amounts and altitudes of SO2 injection during the 1991 Pinatubo eruption. Atmos. Chem. Phys. 23, 921–948. https://doi.org/10.5194/acp-23-921-2023.
Raible, C.C., Brönnimann, S., Auchmann, R., Brohan, P., Frölicher, T.L., Graf, H.-F., Jones, P., Luterbacher, J., Muthers, S., Neukom, R., Robock, A., Self, S., Sudrajat, A., Timmreck, C., Wegmann, M., 2016. Tambora 1815 as a test case for high impact volcanic eruptions: earth system effects. WIREs Clim Change 7, 569–589. https://doi.org/10.1002/wcc.407.
Rampino, M.R., Self, S., 1993. Bottleneck in human-evolution and the toba eruption. Science 262. https://doi.org/10.1126/science.8266085, 1955-1955.
Rasmussen, S.O., Abbott, P.M., Blunier, T., Bourne, A.J., Brook, E., Buchardt, S.L., Buizert, C., Chappellaz, J., Clausen, H.B., Cook, E., Dahl-Jensen, D., Davies, S.M., Guillevic, M., Kipfstuhl, S., Laepple, T., Seierstad, I.K., Severinghaus, J.P., Steffensen, J.P., Stowasser, C., Svensson, A., Vallelonga, P., Vinther, B.M., Wilhelms, F., Winstrup, M., 2013. A first chronology for the North Greenland Eemian Ice Drilling (NEEM) ice core. Clim. Past 9, 2713–2730. https://doi.org/10.5194/cp-9-2713-2013.
Rasmussen, S.O., Bigler, M., Blockley, S.P., Blunier, T., Buchardt, S.L., Clausen, H.B., Cvijanovic, I., Dahl-Jensen, D., Johnsen, S.J., Fischer, H., Gkinis, V., Guillevic, M., Hoek, W.Z., Lowe, J.J., Pedro, J.B., Popp, T., Seierstad, I.K., Steffensen, J.P., Svensson, A.M., Vallelonga, P., Vinther, B.M., Walker, M.J.C., Wheatley, J.J., Winstrup, M., 2014. A stratigraphic framework for abrupt climatic changes during the Last Glacial period based on three synchronized Greenland ice-core records: refining and extending the INTIMATE event stratigraphy. Quat. Sci. Rev. 106, 14–28. https://doi.org/10.1016/j.quascirev.2014.09.007.
Robock, A., 2000. Volcanic eruptions and climate. Rev. Geophys. 38, 191–219. https://doi.org/10.1029/1998rg000054.
Robock, A., Ammann, C.M., Oman, L., Shindell, D., Levis, S., Stenchikov, G., 2009. Did the Toba volcanic eruption of similar to 74 ka BP produce widespread glaciation? J. Geophys. Res. Atmos. 114, D10107. https://doi.org/10.1029/2008jd011652.
Rose, W.I., Newhall, C.G., Bornhorst, T.J., Self, S., 1987. Quaternary silicic pyroclastic deposits of atitlan caldera, Guatemala. J. Volcanol. Geoth. Res. 33, 57–80. https://doi.org/10.1016/0377-0273(87)90054-0.
Savarino, J., Romero, A., Cole-Dai, J., Bekki, S., Thiemens, M.H., 2003. UV induced mass-independent sulfur isotope fractionation in stratospheric volcanic sulfate. Geophys. Res. Lett. 30. https://doi.org/10.1029/2003gl018134.
Scaillet, B., Clemente, B., Evans, B.W., Pichavant, M., 1998. Redox control of sulfur degassing in silicic magmas. J. Geophys. Res. Solid Earth 103, 23937–23949. https://doi.org/10.1029/98jb02301.
Schulz, H., von Rad, U., Erlenkeuser, H., 1998. Correlation between Arabian Sea and Greenland climate oscillations of the past 110,000 years. Nature 393, 54–57. https://doi.org/10.1038/31750.
Schupbach, S., Fischer, H., Bigler, M., Erhardt, T., Gfeller, G., Leuenberger, D., Mini, O., Mulvaney, R., Abram, N.J., Fleet, L., Frey, M.M., Thomas, E., Svensson, A., Dahl-Jensen, D., Kettner, E., Kjaer, H., Seierstad, I., Steffensen, J.P., Rasmussen, S.O., Vallelonga, P., Winstrup, M., Wegner, A., Twarloh, B., Wolff, K., Schmidt, K., Goto-Azuma, K., Kuramoto, T., Hirabayashi, M., Uetake, J., Zheng, J., Bourgeois, J.,

Fisher, D., Zhiheng, D., Xiao, C., Legrand, M., Spolaor, A., Gabrieli, J., Barbante, C., Kang, J.H., Hur, S.D., Hong, S.B., Hwang, H.J., Hong, S., Hansson, M., Iizuka, Y., Oyabu, I., Muscheler, R., Adolphi, F., Maselli, O., McConnell, J., Wolff, E.W., 2018. Greenland records of aerosol source and atmospheric lifetime changes from the Eemian to the Holocene. Nat. Commun. 9. https://doi.org/10.1038/s41467-018-03924-3.

Shane, P., Westgate, J., Williams, M., Korisettar, R., 1995. New geochemical evidence for the youngest toba-tuff in India. Quat. Res. 44, 200–204. https://doi.org/10.1006/qres.1995.1064.

Sigl, M., Fudge, T.J., Winstrup, M., Cole-Dai, J., Ferris, D., McConnell, J.R., Taylor, K.C., Welten, K.C., Woodruff, T.E., Adolphi, F., Bisiaux, M., Brook, E.J., Buizert, C., Caffee, M.W., Dunbar, N.W., Edwards, R., Geng, L., Iverson, N., Koffman, B., Layman, L., Maselli, O.J., McGwire, K., Muscheler, R., Nishiizumi, K., Pasteris, D.R., Rhodes, R.H., Sowers, T.A., 2016. The WAIS Divide deep ice core WD2014 chronology - Part 2: annual-layer counting (0-31 ka BP). Clim. Past 12, 769–786. https://doi.org/10.5194/cp-12-769-2016.

Sigl, M., Winstrup, M., McConnell, J.R., Welten, K.C., Plunkett, G., Ludlow, F., Buntgen, U., Caffee, M., Chellman, N., Dahl-Jensen, D., Fischer, H., Kipfstuhl, S., Kostick, C., Maselli, O.J., Mekhaldi, F., Mulvaney, R., Muscheler, R., Pasteris, D.R., Pilcher, J.R., Salzer, M., Schupbach, S., Steffensen, J.P., Vinther, B.M., Woodruff, T.E., 2015. Timing and climate forcing of volcanic eruptions for the past 2,500 years. Nature 523, 543. https://doi.org/10.1038/nature14565.

Sigl, M., McConnell, J.R., Layman, L., Maselli, O., McGwire, K., Pasteris, D., Dahl-Jensen, D., Steffensen, J.P., Vinther, B., Edwards, R., Mulvaney, R., Kipfstuhl, S., 2013. A new bipolar ice core record of volcanism from WAIS Divide and NEEM and implications for climate forcing of the last 2000 years. J. Geophys. Res. Atmos. 118, 1151–1169. https://doi.org/10.1029/2012jd018603.

Smith, E.I., Jacobs, Z., Johnsen, R., Ren, M., Fisher, E.C., Oestmo, S., Wilkins, J., Harris, J.A., Karkanas, P., Fitch, S., Ciravolo, A., Keenan, D., Cleghorn, N., Lane, C.S., Matthews, T., Marean, C.W., 2018. Humans thrived in South Africa through the Toba eruption about 74,000 years ago. Nature 555, 511. https://doi.org/10.1038/nature25967.

Song, S.R., Chen, C.H., Lee, M.Y., Yang, T.F., Iizuka, Y., Wei, K.Y., 2000. Newly discovered eastern dispersal of the youngest Toba Tuff. Mar. Geol. 167, 303–312. https://doi.org/10.1016/s0025-3227(00)00034-7.

Steffensen, J.P., Andersen, K.K., Bigler, M., Clausen, H.B., Dahl-Jensen, D., Fischer, H., Goto-Azuma, K., Hansson, M., Johnsen, S.J., Jouzel, J., Masson-Delmotte, V., Popp, T., Rasmussen, S.O., Rothlisberger, R., Ruth, U., Stauffer, B., Siggaard-Andersen, M.L., Sveinbjornsdottir, A.E., Svensson, A., White, J.W.C., 2008. High-resolution Greenland Ice Core data show abrupt climate change happens in few years. Science 321, 680–684. https://doi.org/10.1126/science.1157707.

Stocker, T.F., Johnsen, S.J., 2003. A minimum thermodynamic model for the bipolar seesaw. Paleoceanography 18 (4), 1087. https://doi.org/10.1029/2003PA000920.

Storey, M., Roberts, R.G., Saidin, M., 2012. Astronomically calibrated Ar-40/Ar-39 age for the Toba supereruption and global synchronization of late Quaternary records. Proc. Natl. Acad. Sci. U. S. A 109, 18684–18688. https://doi.org/10.1073/pnas.1208178109.

Svensson, A., Bigler, M., Blunier, T., Clausen, H.B., Dahl-Jensen, D., Fischer, H., Fujita, S., Goto-Azuma, K., Johnsen, S.J., Kawamura, K., Kipfstuhl, S., Kohno, M., Parrenin, F., Popp, T., Rasmussen, S.O., Schwander, J., Seierstad, I., Severi, M., Steffensen, J.P., Udisti, R., Uemura, R., Vallelonga, P., Vinther, B.M., Wegner, A., Wilhelms, F., Winstrup, M., 2013. Direct linking of Greenland and Antarctic ice cores at the Toba eruption (74 ka BP). Clim. Past 9, 749–766. https://doi.org/10.5194/cp-9-749-2013.

Thomason, L.W., Ernest, N., Millan, L., Rieger, L., Bourassa, A., Vernier, J.P., Manney, G., Luo, B.P., Arfeuille, F., Peter, T., 2018. A global space-based stratospheric aerosol climatology: 1979-2016. Earth Syst. Sci. Data 10, 469–492. https://doi.org/10.5194/essd-10-469-2018.

Timmreck, C., Graf, H.F., Zanchettin, D., Hagemann, S., Kleinen, T., Kruger, K., 2012. Climate response to the Toba super-eruption: regional changes. Quat. Int. 258, 30–44. https://doi.org/10.1016/j.quaint.2011.10.008.

Toohey, M., Kruger, K., Schmidt, H., Timmreck, C., Sigl, M., Stoffel, M., Wilson, R., 2019. Disproportionately strong climate forcing from extratropical explosive volcanic eruptions. Nat. Geosci. 12, 100. https://doi.org/10.1038/s41561-018-0286-2.

Toohey, M., Sigl, M., 2017. Volcanic stratospheric sulfur injections and aerosol optical depth from 500 BCE to 1900 CE. Earth Syst. Sci. Data 9, 809–831. https://doi.org/10.5194/essd-9-809-2017.

Von Rad, U., Burgath, K.P., Pervaz, M., Schulz, H., 2002. Discovery of the Toba Ash (C. 70 Ka) in a High-Resolution Core Recovering Millennial Monsoonal Variability off Pakistan. Meeting of the Geological-Society-of-London, Piccadilly, England, pp. 445–461. https://doi.org/10.1144/gsl.Sp.2002.195.01.25. Apr 04-05, WOS: 000181985300025.

Wolff, E.W., Chappellaz, J., Blunier, T., Rasmussen, S.O., Svensson, A., 2010. Millennial-scale variability during the last glacial: the ice core record. Quat. Sci. Rev. 29, 2828–2838. https://doi.org/10.1016/j.quascirev.2009.10.013.

Yang, Q., Mayewski, P.A., Zielinski, G.A., Twickler, M., Taylor, K.C., 1996. Depletion of atmospheric nitrate and chloride as a consequence of the Toba volcanic eruption. Geophys. Res. Lett. 23, 2513–2516. https://doi.org/10.1029/96gl02201.